IOPscience iopscience.iop.org

Home Search Collections Journals About Contact us My IOPscience

Vibrational properties of elemental hydrogen centres in Si, Ge and dilute SiGe alloys

This article has been downloaded from IOPscience. Please scroll down to see the full text article.

2005 J. Phys.: Condens. Matter 17 S2155

(http://iopscience.iop.org/0953-8984/17/22/002)

View the table of contents for this issue, or go to the journal homepage for more

Download details:
IP Address: 129.252.86.83
The article was downloaded on 28/05/2010 at 04:54

Please note that terms and conditions apply.

INSTITUTE OF PHYSICS PUBLISHING JOURNAL OF PHYSICS: CONDENSED MATTER

J. Phys.: Condens. Matter **17** (2005) S2155–S2164 doi:10.1088/0953-8984/17/22/002

Vibrational properties of elemental hydrogen centres in Si, Ge and dilute SiGe alloys

A Balsas[1], V J B Torres[1], J Coutinho[1], R Jones[2], B Hourahine[3], P R Briddon[4] and M Barroso[1]

[1] Department of Physics, University of Aveiro, 3810 Aveiro, Portugal
[2] School of Physics, University of Exeter, Stocker Road, Exeter EX4 4QL, UK
[3] Department of Physics, Universität Paderborn, Warburger Street 100, D-33098 Paderborn, Germany
[4] School of Natural Sciences, University of Newcastle upon Tyne, Newcastle upon Tyne NE1 7RU, UK

E-mail: coutinho@fis.ua.pt

Received 6 October 2004, in final form 6 December 2004
Published 20 May 2005
Online at stacks.iop.org/JPhysCM/17/S2155

Abstract
The local vibrational modes arising from single interstitial hydrogen centres in Si, Si-rich SiGe, Ge-rich SiGe, and Ge crystals are modelled by an *ab initio* supercell method. The stress response of the 1998 and 1794 cm^{-1} bands that appear in proton-implanted Si and Ge samples is well reproduced, further confirming their assignment to bond-centred H^+ defects. It is shown that H^- in Ge is anti-bonded to a Ge atom, and is likely to be considerably less mobile than in Si. Although H^+ is not trapped by the minority species in both Si-rich and Ge-rich alloys, we find that H^- can be stabilized by forming anti-bonded H–Si structures.

1. Introduction

Because of its high diffusion rate and reactivity, as well as its occurrence in many chemical sources used in growth and processing, hydrogen is an important defect in semiconductors. It is well known that hydrogen can dramatically modify their electrical and optical properties by passivating, displacing or even activating electrical levels through the formation of hydrogen–impurity complexes [1–3]. Isolated hydrogen in silicon has been widely studied both experimentally and theoretically. Under equilibrium conditions it can occur in two charge states, i.e., positive and negative, depending on the Fermi level position, and it shows a negative-U behaviour [4]. This has been confirmed by several experimental studies. Deep level transient spectroscopy (DLTS) and capacitance transient measurements [5–8] have assigned $(-/0)$ and $(0/+)$ levels to isolated H in Si at around $E_c - 0.5$ eV and $E_c - 0.17$ eV, respectively. The neutral state is metastable, and may be produced under white light illumination of p-type

Si [9, 10]. These observations are correlated with the behaviour of the *muonium* (a pseudo-isotope of hydrogen), where four types of muonium centres have been reported to form at low temperatures, namely paramagnetic stable Mu^0_{BC} and metastable Mu^0_{Td}, as well as diamagnetic Mu^+_{BC} and Mu^-_{Td}, where the BC and Td subscripts stand for their bond-centred and tetrahedral interstitial location [11, 12].

From the many theoretical and experimental investigations into isolated hydrogen in Si, it is now accepted that positive and negative hydrogen ions sit at the bond-centre, H^+_{BC}, and tetrahedral interstitial (or a slightly distorted), H^-_{Td}, lattice sites, respectively. Neutral atoms find their ground state at the bond-centre site, H^0_{BC}, and are metastable at the tetrahedral interstitial location, H^0_{Td} [13, 14].

In situ local vibrational mode (LVM) infrared spectroscopy on low-T proton-implanted Si has revealed that H^+_{BC} gives rise to an absorption band at 1998 cm^{-1}, assigned to an A_{2u} asymmetric stretching oscillation mainly localized on the Si–H–Si unit [15]. On the other hand, no vibrational bands have been detected that could be assigned to H^-_{Td} in Si, suggesting the absence of any strong Si–H bonds in the defect.

Similar measurements were carried out on Ge samples implanted with protons at low T [16]. Besides a prominent vibrational band at 1794 cm^{-1} identified as H^+_{BC}, other bands associated with isolated H were detected at 745, 1480 and 1488 cm^{-1}. From the stress-splitting pattern under a polarized light source, the 745 cm^{-1} band was assigned to a doubly degenerate Ge–H bend-mode arising from a H^-_{AB}, whereas the other two bands are most likely to be overtones of the bend-mode which are split by anharmonic coupling. It is important to note that this assignment implies the existence of a $(-/0)$ level, or as we shall see below, a $(-/+)$ state like in Si. However, as pointed out in [16], unless the Ge–H structure responsible for the 745 cm^{-1} band has a non-covalent character, a high-frequency stretch mode should also have been detected. This is a puzzling feature which is still not understood.

Laplace-DLTS measurements by Dobaczewski *et al* [17] on n-doped Ge, prepared in a way similar to the *in situ* infrared absorption study, concluded that a metastable $H_{BC}(0/+)$ level in Ge lies 0.11 eV below the conduction band bottom. The emission rate splitting pattern from uniaxially stressed samples indicates a trigonal defect, while annealing studies under reverse-bias, where the defect is positively charged, show the same thermal stability (∼220 K) as the 1794 cm^{-1} band. This shows that the 1794 cm^{-1} band is due to H^+. Unfortunately no acceptor state has been detected by minority carrier injection, implying that if there is a $(-/0)$ state, it either lies close to mid-gap, or more likely, it is very shallow or even resonant with the valence states in agreement with earlier theoretical studies [18, 19]. These investigations placed H^- at the tetrahedral interstitial site. However, we believe that this model is not compatible with the observation of the 745 cm^{-1} bend-mode, and hence we reinvestigate this problem below.

The effect of alloying Si and Ge species on the properties of interstitial H is of current interest. Low-T *in situ* Laplace-DLTS in H-implanted Si-rich alloys [20] has demonstrated a Ge-perturbed $H_{BC}(0/+)$ level, denoted as E3′(Ge), which could be distinguished from the dominant E3′ peak associated with isolated H_{BC} in Si [21, 6]. It was found that the emission enthalpy and formation barrier of E3′(Ge) are only 17 and 13 meV lower than those of E3′, respectively. Moreover, the formation energy of the E3′(Ge) defect is ∼0.2 meV higher than that of E3′ in both positive and neutral states. E3′(Ge) was then assigned to a H–Ge pair coupled through a Si atom [20]. The structure is hereafter labelled H_{BC2}, and is shown in figure 1.

The results from the electrical measurements in SiGe described above are supported by Fourier transform infrared data [22]. Accordingly, in Si-rich alloys (Ge fraction $x = 0.0025$) at least two absorption bands, L1 at 1997 cm^{-1} and L2 at 2004 cm^{-1}, with similar annealing behaviour to the 1998 cm^{-1} band in Si, were detected. These were assigned to Ge-free Si–

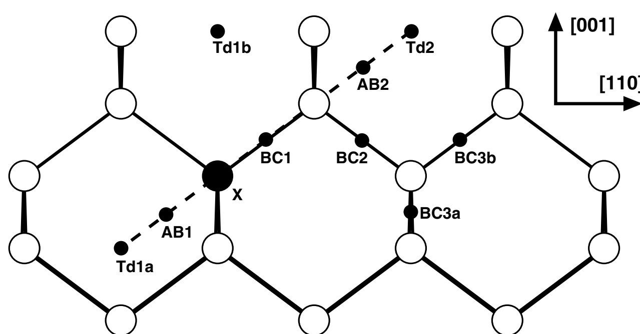

Figure 1. Configurations of interstitial H (small dots) in Si (Ge). Host atoms are shown as white circles. A substitutional X = Ge (Si) atom is represented by the black circle. Hydrogen sites are labelled according to the usual notation, where BC, AB and Td stand for bond-centred, anti-bonded and tetrahedral interstitial sites, respectively. It should be noted that BC and AB structures produce large lattice relaxations that are not shown (see text).

H^+_{BC}–Si, and Ge-perturbed Si–H^+_{BC}–Si units, respectively. The slightly enhanced L2 frequency suggests that H lies in a *compressed* Si–Si bond due to the presence of a nearby Ge atom.

This paper extends the work of [23] and we compare the vibrational properties of stable H^+ and H^- interstitial defects in Si, Si-rich SiGe, Ge-rich SiGe and Ge crystals using density functional based supercell calculations. Before describing our results and conclusions, we will briefly summarize our computational method.

2. Theoretical details

We employ a density functional code (AIMPRO) [24] incorporating a Padé parameterization of the exchange–correlation energy and potential [25]. Core states are avoided by employing the dual-space separable pseudopotentials by Hartwigsen *et al* [26]. Valence wavefunctions are represented with Cartesian–Gaussian s-, p- and d-type sets of functions [27], and the Hartree and exchange–correlation terms are calculated in reciprocal space using up to 200 Ryd plane-waves. The present method has been successful in accurately describing defect properties in SiGe alloys [27].

Hydrogen in Si, Ge and dilute SiGe alloys was modelled by selectively placing H^+ and H^- ions in Si_{64}, Ge_{64}, $Si_{63}Ge_1$ and Si_1Ge_{63} cubic supercells (see figure 1). The last two represent alloys with 1.56% and 98.4% Ge concentration, respectively. All atomic and electronic degrees of freedom were allowed to relax, together with the cubic lattice parameter, in order to minimize the total energy. The Brillouin zone was sampled with a total of 8 (MP-2^3) special **k**-points [28]. Using this level of theory we obtain 5.3947 Å (5.5821 Å) and 97.0 GPa (73.5 GPa) for the lattice constant a_0 and bulk modulus B of Si (Ge), respectively. These are no more than ∼1% and ∼4% away from the measured values for a_0 and B, respectively. The lattice constants of $Si_{63}Ge_1$ and Si_1Ge_{63} supercells were respectively 5.3973 and 5.5792 Å [27].

As shown in figure 2(a), the calculated Kohn–Sham band-gap of bulk Ge is only 0.33 eV at Γ. This contrasts with the measured 0.74 eV indirect gap, with the bottom of the conduction band lying at the edge of the zone along ⟨111⟩. This well known discrepancy demonstrates the limitations of the treatment of correlation terms. Therefore, special attention was paid to the way electron levels were occupied, in particular, to make sure that the donor band in H^+ does not fall below the valence band top, and the acceptor band in H^- does not resonate with the conduction band.

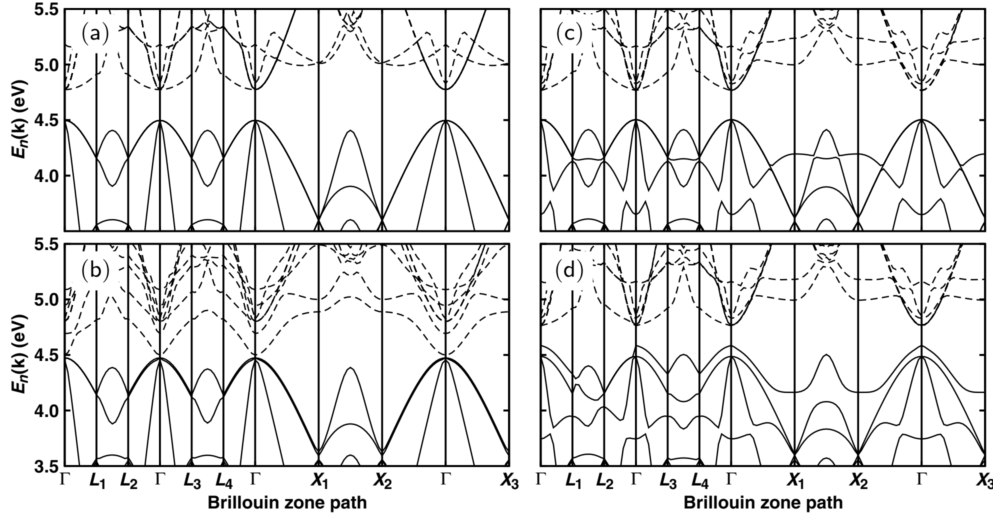

Figure 2. One-electron (Kohn–Sham) band structures for (a) 64 Ge atom bulk supercell with cube edge L = 2 a_0, where a_0 = 5.5821 Å is the Ge lattice constant, and for similar cells containing (b) H_{BC}^+, (c) H_{Td}^-, and (d) H_{AB}^-. The Brillouin zone path goes between Γ, the MP-2^3 **k**-points ($L_1, \ldots, L_4$), and X_1, X_2 and X_3 (($\frac{1}{2}$, 0, 0), (0, $\frac{1}{2}$, 0), (0, 0, $\frac{1}{2}$), respectively, in units of $2\pi/L$). Solid and dashed lines represent occupied and empty bands, respectively.

Local vibrational mode frequencies were calculated from numerical second derivatives taken from the *ab initio* code. These were calculated by displacing the H atom and its immediate neighbours along all six Cartesian directions. The effect of uniaxial stress on the stretch frequency ω_H of trigonal H_{BC}^+ defects in Si and Ge were also investigated. Accordingly, under the effect of an arbitrary stress σ or strain $\epsilon = s \cdot \sigma$, respectively, a vibrational frequency shifts by $\mathrm{Tr}(A \cdot \sigma) = \mathrm{Tr}(B \cdot \epsilon)$. Here A and B are the so-called *piezospectroscopic* strain and stress tensors, respectively [29], s is the compliance tensor of the host material, and σ is positive for tensile stress. For a trigonal defect, A (and B) may be expressed by diagonal A_1 (B_1) and off-diagonal A_2 (B_2) Cartesian components only. These were computed from the ω_H values obtained after deforming $Si_{64}H_{BC}^+$ and $Ge_{64}H_{BC}^+$ supercells. Two different deformations, $\epsilon_{ij} = e\delta_{i1}\delta_{1j}$ and $\epsilon_{ij} = \frac{1}{2}e(\delta_{i1}\delta_{2j} + \delta_{i2}\delta_{1j})$ were applied, such that

$$A_1 = (s_{11} + 2s_{12})\frac{\partial\omega_H}{\partial e},$$

and

$$A_2 = s_{44}\frac{\partial\omega_H}{\partial e},$$

respectively. Components A_1 and A_2 quantify the rate change of ω_H under purely uniaxial and shear stress. We used the measured elastic compliance tensor s for Si, $s_{11} = 7.68 \times 10^{-3}$ GPa^{-1}, $s_{12} = -2.14 \times 10^{-3}$ GPa^{-1} and $s_{44} = 12.6 \times 10^{-3}$ GPa^{-1}, and for Ge, $s_{11} = 9.69 \times 10^{-3}$ GPa^{-1}, $s_{12} = -2.51 \times 10^{-3}$ GPa^{-1} and $s_{44} = 14.8 \times 10^{-3}$ GPa^{-1}.

3. Results

We considered the isolated hydrogen atom at the different sites shown in figure 1. The black central atom X represents a minority species in the SiGe alloy. Because of the negative-U

character of the centre, and based on previous works, we report results for negative (Td or a nearby site) and positive (BC site) charge states only.

3.1. H in elemental Si and Ge crystals

Let us start with isolated H defects in elemental Si (Ge) crystals. In line with other reports we find the Si–H (Ge–H) bond lengths for H_{BC}^{+} to be 1.587 Å (1.640 Å), producing a strong outward displacement of the nearest pair of Si (Ge) atoms. Their separation increases by about 36% (36%) when compared to bulk Si (Ge). H_{BC}^{0} has a paramagnetic gap state that is nodal on H, and made up of an anti-bonding combination of its nearest Si hybrid orbitals. In figure 2(b) we depict the one-electron band structure for H_{BC}^{+} in Ge. As expected for an anti-bonding state, the lowest unoccupied band has a strong conduction band character. A similar picture applies to the analogous defect in Si.

For negatively charged H in Si we find that the energy of the AB configuration is only 0.01 eV below that of Td. In the AB form, the H atom is 1.794 and 0.132 Å away from its nearest Si atom and from the tetrahedral site, respectively. Hence we may conclude that even at cryogenic temperatures the interstitial H^- will show an *effective* tetrahedral symmetry. Interestingly, H seems to behave differently in Ge. The AB structure is now about 0.1 eV more stable than Td, producing a considerable distortion to the Ge lattice, and leading to a Ge–H_{AB}^{-} bond length of 1.702 Å. This is considerably larger than the 1.52 Å Ge–H bonds in germane (GeH_4), and mirrors a large departure from the sp^3-like bond. The above-mentioned energetics ignores zero-point energy contributions of ∼0.1 eV. Nevertheless, while the Si–Si distance in the H_{AB}^{-}–Si–Si axial unit barely changes with respect to the bulk bond length, the Ge–Ge bond along the trigonal axis in H_{AB}^{-}–Ge–Ge increases by about 10% with respect to the bulk bond-length.

The band structures of H_{Td}^{-} and H_{AB}^{-} in Ge are shown in figures 2(c) and (d), respectively. They are consistent with the DLTS measurements [17], showing that H_{AB} and H_{BC} in Ge exhibit shallow acceptor and deep donor activity respectively. The existence of a bound H_{AB} form in Ge may have consequences for the diffusivity of H^-. To investigate this, we calculated the total energies of H^- at the hexagonal site (H_{Hex}^{-}). In figure 1, this lies half-way between any two of the host atoms at opposite corners of the skewed hexagons. Our calculations indicate that the energy of H_{Hex}^{-} defects in Si and Ge are 0.40 and 0.55 eV, respectively, above the ground state H_{AB}^{-}. Assuming the H_{Hex}^{-} structure as being close to the saddle-point between two neighbouring Td sites, and considering the difference in zero-point energies, our calculations indicate that the migration barrier of H^- in Ge is 0.1 eV lower than in Si.

The calculated local vibrational mode frequencies for the BC and AB forms of H^+ and H^-, respectively, in Si and Ge supercells are shown in table 1. The bond-centred H^+ defect in Si (Ge) produces a high-frequency A_{2u} mode due to the asymmetric stretch oscillation of the Si(Ge)–H–Si(Ge) unit. As expected, by neglecting anharmonic effects, these frequencies are about 100 cm^{-1} above the measured data. The same applies to the isotope data. We expect that anharmonic corrections will be less important when H is substituted by the heavier deuterium atom, and therefore $\delta\omega_D$ values are no more than ∼50 cm^{-1} above the measured data. Turning now to AB structures, these give rise to A_1 stretch and E bend modes. In Si these differ by only 150 cm^{-1}, which mirrors the similarity between AB and Td forms. To our knowledge, no vibrational band associated with this defect has been reported so far. Perhaps a rapid thermal motion between equivalent AB and Td sites makes any resulting mode short lived, and therefore difficult to detect.

Now for Ge:H_{AB}^{-}, the A_1 and E modes are found at 1239 and 704 cm^{-1}. We note that the bend-mode frequency is underestimated when compared to the 745 cm^{-1} band assigned

Table 1. Vibrational mode frequencies (ω_H), and their downward shifts for deuterium ($\delta\omega_D$), for H_{BC}^+ and H_{AB}^- in pure Si and Ge supercells. Experimental values [15, 16] are shown within parentheses. All values are given in cm^{-1}.

	Si:H_{BC}^+	Si:H_{AB}^-		Ge:H_{BC}^+	Ge:H_{AB}^-	
Symmetry	A_{2u}	E	A_1	A_{2u}	E	A_1
ω_H	2125	686	840	1897	704	1239
	(1998)	—	—	(1794)	(745)	—
$\delta\omega_D$	613	196	246	552	206	361
	(549)	—	—	(501)	(210)	—

to H_{AB}^- in Ge [16]. It is instructive to compare the results for Ge:H_{AB}^- with those for the H_2^* complex [30]. The latter defect is a pair of interstitial H atoms, forming anti-bonding and nearly bond-centred units, respectively. The anti-bonding unit has been linked to E-bend and A_1-stretch absorption bands at 765 and 1773.8 cm^{-1}, and we obtain these at 722 and 1717.8 cm^{-1}, respectively. The ~60 cm^{-1} error on the latter frequency suggests that the stretch frequency of Ge:H_{AB}^- lies around 1300 cm^{-1}, and not at 1770 cm^{-1} as suggested in [16].

The piezospectroscopic tensors for the stretch frequencies of H_{BC}^+ forms were calculated following the procedure described in section 2. In Si, for the 2125 cm^{-1} mode we find $A_1 = -11.0$ cm^{-1} GPa^{-1} and $A_2 = -12.5$ cm^{-1} GPa^{-1}. These agree well with the observed uniaxial stress response of the 1998 cm^{-1} band where $A_1 = -9$ cm^{-1} GPa^{-1} and $A_2 = -11$ cm^{-1} GPa^{-1}. For the 1897 cm^{-1} mode in Ge, we find A_1 to be -12.7 cm^{-1} GPa^{-1} and $A_2 = -14.4$ cm^{-1} GPa^{-1}, which can be compared with experimental values of -11.1 cm^{-1} GPa^{-1} and -13 cm^{-1} GPa^{-1}, respectively[5].

We may express A along the principal directions of a trigonal defect. Accordingly $A_\parallel = A_1 + 2A_2$ and $A_\perp = A_1 - A_2$ represent the shift rate of ω_H when the defect is under stress along and perpendicular to its trigonal axis. For Si, $A_\parallel = -36.0$ cm^{-1} GPa^{-1} and $A_\perp = 1.5$ cm^{-1} GPa^{-1}, whereas for Ge, $A_\parallel = -41.5$ cm^{-1} GPa^{-1} and $A_\perp = 1.7$ cm^{-1} GPa^{-1}. These imply that the effect of stress perpendicular to the Si–H–Si (Ge–H–Ge) unit is negligible when compared to when it is aligned along the [111] symmetry axis.

3.2. Hydrogen interaction with dilute species in SiGe

Now we turn to the interaction between H and a Ge atom in Si-rich SiGe, or a Si atom in Ge-rich SiGe. All structures investigated are depicted in figure 1, and their total energies are reported in table 2. Here, the energies of positively and negatively charged complexes are given relative to H_{BC}^+ and H_{Td}^- defects at a remote location to the minority elemental species X, being represented by $H_{BC}^+ + X$ and $H_{Td}^- + X$, respectively.

It is striking to note that, in the positive charge state, all configurations (including H_{BC1}^+), are degenerate within the accuracy of the method. In $Si_{63}Ge_1$ supercells, the H_{BC}^+–Si bond lengths mostly shorten (down to 1.567 Å in BC1 form) as H approaches the Ge atom, whereas in Si_1Ge_{63}, the H_{BC}^+–Ge bond lengths are mostly elongated (up to 1.670 Å in BC1 form) as H approaches the Si atom. This trend follows from the compressive and tensile character of Ge and Si impurities in Si and Ge crystals, respectively.

Despite the small energy differences between all BC sites, it is likely that there is a slight preference to form X-perturbed H centres in low-temperature proton-implanted dilute

[5] In [16] the authors assume a convention where tensile stress is negative. Consequently, they report A_1 and A_2 components with opposite signs to those reported here.

Table 2. Energies (eV) of interstitial H^+ (H^-) defects relative to H^+_{BC} (H^-_{Td}) at a remote location to a substitutional species X in a 64 atom cell [denoted as $H^+_{BC} + X$ ($H^-_{Td} + X$)]. Here X = Ge in $Si_{63}Ge_1$ or X = Si for Si_1Ge_{63} supercells. Non-numerical cells refer to the final structure after full relaxation. All configurations are labelled according to figure 1.

Defect	$Si_{63}Ge_1$	Si_1Ge_{63}
$H^+_{BC} + X$	0.00	0.00
H^+_{BC1}	0.00	−0.01
H^+_{BC2}	0.00	0.00
H^+_{BC3a}	0.00	0.00
H^+_{BC3b}	0.01	−0.01
$H^-_{Td} + X$	0.00	0.00
H^-_{AB1}	Td1a	−0.37
H^-_{AB2}	−0.11	Td2
H^-_{Td1a}	0.06	AB1
H^-_{Td1b}	0.02	−0.03
H^-_{Td2}	AB2	0.01

SiGe samples, as a greater density is found for $E3'$(Ge) than expected from purely random statistics [20]. Moreover, a mobile H^- species in Si may be trapped near a Ge atom in Si-rich SiGe to form H^-_{AB2}. For a fractional Ge content $x = 1/64$ the average Si–Ge bond length is 2.370 Å [27], and these are softer than Si–Si ones. This difference, along with the fact that Si–H bonds are stronger than Ge–H bonds, suggests the formation of the Ge–Si–H^-_{AB2} structure in proton-implanted Si-rich SiGe. For similar reasons, the ground state of H^- in Si_1Ge_{63} shows a direct H–Si bond, producing a H^-_{AB1}–Si–Ge unit along ⟨111⟩ (see figure 1). Now the Ge–Ge bonds are softer than Si–Ge ones, and in contrast to H^-_{AB} defects in Ge, Si–Ge–H^-_{AB2} complexes are unstable and relax to H^-_{Td2}.

Table 3 shows the calculated local vibrational frequencies of H–Ge (H–Si) defects in $Si_{63}Ge_1$ (Si_1Ge_{64}) supercells corresponding to a fractional Ge (Si) concentration of 1.6%. The top row gives the frequencies of H^+_{BC} at a remote location to the minor species X present in the same supercell. These are 2109 cm^{-1} (1897 cm^{-1}) for Si-rich (Ge-rich) cells and will be used as a reference for other concentrations.

Let us first look at modes arising from Si–H–Ge units in Si- and Ge-rich alloys. In these BC1 forms, H makes a stronger bond with the Si atom, and as expected, their frequencies (see table 3) lie below (above) those from Si–H–Si (Ge–H–Ge) defects in $Si_{63}Ge_1$ (Si_1Ge_{63}) supercells.

A substitutional Ge atom in Si (Si atom in Ge) produces an isotropic compressive (tensile) strain field centred on its site. The calculated Si–Si bond lengths around a substitutional Ge atom in Si are 2.3330, 2.3370, 2.3346 Å for BC2, BC3a and BC3b bonds, respectively, which are compressed when compared with the remote 2.3372 Å Si–Si bonds. Looking at table 3, we conclude that the ω_H frequencies are correlated with the available space for H between Si atoms. BC2 and BC3b sites lie on compressed bonds and consequently H^+_{BC2} and H^+_{BC3b} have LVM frequencies (2123 and 2119 cm^{-1}, respectively) above that of $H^+_{BC} + Ge_s$ (2109 cm^{-1}). On the other hand, BC3a lies on a less strained bond, and hence its frequency is just below that of $H^+_{BC} + Ge_s$.

Analogously, for Ge-rich alloys, the calculated bond lengths around a Ge:Si_s defect are 2.4285, 2.4160, 2.4179 Å for BC2, BC3a and BC3b bonds, respectively, and now they are

Table 3. Vibrational stretch frequencies for hydrogen and deuterium defects (ω_H and ω_D, respectively) located at bond-centre and anti-bond sites near to Ge_s or Si_s centres in $Si_{63}Ge_1$ and Si_1Ge_{63} supercells, respectively (defect labeling according to figure 1). Non-numerical cells refer to the final structure after full relaxation. All values are in cm^{-1}.

	$Si_{63}Ge_1$		Si_1Ge_{63}	
Defect	ω_H	ω_D	ω_H	ω_D
$H^+_{BC} + X$	2109	1501	1897	1345
H^+_{BC1}	2091	1485	1936	1376
H^+_{BC2}	2123	1510	1887	1338
H^+_{BC3a}	2108	1500	1899	1346
H^+_{BC3b}	2119	1508	1892	1341
H^-_{AB1}	Td1a	Td1a	1449	1035
H^-_{AB2}	1063	755	Td2	Td2

elongated with respect to the remote 2.4159 Å Ge–Ge bonds. Again, these correlate well with the LVM frequencies of H^+ on these sites. Strong tensile strain on BC2 and BC3b bonds lower the frequencies of H^+_{BC2} and H^+_{BC3b} defects, whereas the weak distortion on BC3a leaves the stretch frequency of H^+_{BC3b} almost unchanged with respect to that of $H^+_{BC} + Si_s$, respectively.

Finally we comment on frequencies of AB defects. Despite H^-_{AB2} in $Si_{63}Ge_1$ possessing the similar Si–H structure shown by H^-_{AB1} in Si_1Ge_{63}, the latter produces a Si–H stretching frequency about 400 cm^{-1} higher. Negatively charged H in Si is highly mobile and difficult to detect. However, considering the stability of H^-_{AB1} in Si_1Ge_{63} as well as the location of its stretch frequency, we expect this defect to produce a detectable vibrational absorption band in low-T proton-implanted Ge-rich samples.

4. Conclusions

The results of a density functional study of the structure and vibrational modes of interstitial H^+ and H^- defects in Si and Ge crystals, as well as their interaction with Ge (Si) atoms in Si-rich (Ge-rich) SiGe alloys, have been described. While positively charged BC forms have analogous properties in Si and Ge crystals, hydrogen in the negative charge state is expected to be less mobile in Ge than in Si. While H^-_{AB} and H^-_{Td} in Si show nearly the same structure and energetics, in Ge, H^-_{AB} is more stable by about 0.1 eV.

The calculated LVM frequencies of H^+_{BC} defects in Si and Ge exceed the 1998 and 1794 cm^{-1} observed bands by $\sim$100 cm^{-1}. The error is probably largely a consequence of anharmonic contributions. The stress response of these A_{2u} modes was investigated and piezospectroscopic tensor A found to be in excellent agreement with experimental values [16]. We show that while the frequency barely changes when stress is perpendicular to the trigonal symmetry axis, it is strongly enhanced when stress is along the same axis.

The E and A_1 mode frequencies arising from the stable H^-_{AB} defect in Ge are placed at 704 and 1239 cm^{-1}, respectively. The first frequency is in fair agreement with the reported experimental value at 745 cm^{-1} band, but the stretch mode remains undetected.

In agreement with previous theory [23], our results indicate that H^+_{BC} in SiGe does not form an energetically favoured structure. All bond-centred configurations are degenerate within the accuracy of the method. DLTS measurements have resolved a Si–H–Si defect perturbed by Ge [20]. The density of this defect is 12.5% greater than expected for a random population.

Whilst we cannot rule out that the formation barrier of $E3'$(Ge) (assigned to H^+_{BC2}) is reduced in comparison to that of $E3'$ [20], we have to consider that several Ge-perturbed H_{BC} defects with similar traps are contributing to the $E3'$(Ge) signal.

We also found that H^- ions may be trapped at low temperatures in the form of H^-_{AB}–Si–Ge units in dilute SiGe alloys. In a Si-rich host, the presence of *soft* Si–Ge bonds, when compared to the abundant and *stiff* Si–Si bonds, encourages the formation of Si–H bonds at the expense of the Si–Ge ones. On the other hand, in Ge-rich alloys, H^-_{AB}–Si defects are about 0.27 eV more stable than the isolated H^-_{AB}–Ge defect. The former defects, in particular H^-_{AB1} in Ge-rich material, give rise to stretch mode frequencies well above the Raman edge. The fact that these defects are bound by a few tenths of an eV leads us to believe that they should be present and could be detected by infrared absorption as well as by DLTS measurements.

Finally, we report on the local vibrational modes of H^+_{BC} complexes in Si-rich and Ge-rich alloys, with nearby minority species X. Our results indicate that there are clear trends for the asymmetric stretch mode frequency, resulting from the local strain produced by X. In Si-rich material, Ge-perturbed Si–H^+_{BC}–Si LVM frequencies tend to lie above the frequency from the analogous Ge-free complex. Analogously, in Ge-rich SiGe, Si atoms produce a tensile strain field, and Ge–H^+_{BC}–Ge LVM frequencies now tend to lie below the frequency from the Si-free complex.

Acknowledgments

The authors would like to thank B Bech Nielsen, R N Pereira and L Dobaczewski for their useful comments and criticisms.

References

[1] Pearton S J, Corbett J W and Stavola M 1992 *Hydrogen in Crystalline Semiconductors* (Berlin: Springer)
[2] Pankove J I and Johnson N M (ed) 1991 *Hydrogen in Semiconductors* (*Semiconductors and Semimetals* vol 34) (Boston, MA: Academic)
[3] Nickel N H (ed) 1999 *Hydrogen in Semiconductors II* (*Semiconductors and Semimetals* vol 61) (New York: Academic)
[4] Van de Walle C G, Bar-Yam Y and Pantelides S T 1988 *Phys. Rev. Lett.* **60** 2761–4
[5] Johnson N M, Herring C and Van de Walle C G 1994 *Phys. Rev. Lett.* **73** 130
[6] Holm B, Bonde Nielsen K and Bech Nielsen B 1991 *Phys. Rev. Lett.* **66** 2360–3
[7] Bonde Nielsen K, Beck Nielsen B, Hansen J, Andersen E and Andersen J U 1999 *Phys. Rev.* B **60** 1716
[8] Bonde Nielsen K, Dobaczewski L, Sogard S and Beck Nielsen B 2002 *Phys. Rev.* B **65** 075205
[9] Gorelkinskii Yu V and Nevinnyi N N 1987 *Pis. Zh. Tekh. Fiz.* **13** 105
Gorelkinskii Yu V and Nevinnyi N N 1987 *Sov. Tech. Phys. Lett.* **13** 45 (Engl. Transl.)
Gorelkinskii Yu V and Nevinnyi N N 1991 *Physica* B **170** 155
[10] Bech Nielsen B, Bonde Nielsen K and Byerger J R 1994 *Mater. Sci. Forum* **143–147** 909
[11] Patterson B D 1988 *Rev. Mod. Phys.* **60** 69
[12] Hitti B, Kreitzman S R, Estle T L, Bates E S, Dawdy M R, Head T L and Lichti R L 1999 *Phys. Rev.* B **59** 4918
[13] Estreicher S K 1995 *Mater. Sci. Eng.* R **14** 319
[14] Jones R, Coomer B J, Hourahine B and Resende A 2000 *Solid State Phenom.* **71** 173
[15] Budde M 1998 Hydrogen-related defects in proton implanted silicon and germanium *PhD Thesis* Århus Center for Atomic Physics, University of Århus, Denmark
[16] Budde M, Beck Nielsen B, Parks Cheney C, Tolk N H and Feldman L C 2000 *Phys. Rev. Lett.* **85** 2965
[17] Dobaczewski L, Bonde Nielson K, Zangberg N, Bech Nielson B, Peaker A R and Markevich V P 2004 *Phys. Rev.* B **69** 245207
[18] Denteneer P J H, Van de Walle C G and Pantelides S T 1989 *Phys. Rev. Lett.* **62** 1884
[19] Estreicher S K, Roberson M A and Maric Dj M 1994 *Phys. Rev.* B **50** 17018
[20] Bonde Nielsen K, Dobaczewski L, Peaker A R and Abrosimov N V 2003 *Phys. Rev.* B **68** 045204
[21] Irmsher K, Klose H and Maass K 1984 *J. Phys. C: Solid State Phys.* **17** 6317

[22] Pereira R N, Dobaczewski L and Bech Nielsen B 2003 *Physica* B **340–342** 803
[23] Hourahine B, Jones R, Öberg S, Briddon P R and Frauenheim T 2003 *J. Phys.: Condens. Matter* **15** S2803
[24] Briddon P R and Jones R 2000 *Phys. Status Solidi* b **207** 131
[25] Goedecker S, Teter M and Hutter J 1996 *Phys. Rev.* B **54** 1703
[26] Hartwigsen C, Goedecker S and Hutter J 1998 *Phys. Rev.* B **58** 3641
[27] Balsas A, Coutinho J, Torres V J B, Briddon P R and Barroso M 2004 *Phys. Rev.* B **70** 085201
[28] Monkhorst H J and Pack J D 1976 *Phys. Rev.* B **13** 5188
[29] Kaplyanskii A A 1964 *Opt. Spectrosc.* **16** 329
[30] Budde M, Bech Nielsen B, Jones R, Goss J and Öberg S 1996 *Phys. Rev.* B **54** 5485